Environment, Development and Sustainability
https://doi.org/10.1007/s10668-021-01402-3

Surface tension of binary mixtures containing environmentally friendly ionic liquids: Insights from artificial intelligence

Roy Setiawan[1] · Reza Daneshfar[2] · Omid Rezvanjou[2] · Siavash Ashoori[2] · Maryam Naseri[3]

Received: 10 October 2020 / Accepted: 2 April 2021

Abstract
The surface tension (ST) of ionic liquids (ILs) and their accompanying mixtures allows engineers to accurately arrange new processes on the industrial scale. Without any doubt, experimental methods for the specification of the ST of every supposable IL and its mixtures with other compounds would be an arduous job. Also, experimental measurements are effortful and prohibitive; thus, a precise estimation of the property via a dependable method would be greatly desirable. For doing this task, a new modeling method according to artificial neural network (ANN) disciplined by four optimization algorithms, namely teaching–learning-based optimization (TLBO), particle swarm optimization (PSO), genetic algorithm (GA) and imperialist competitive algorithm (ICA), has been suggested to estimate ST of the binary ILs mixtures. For training and testing the applied network, a set of 748 data points of binary ST of IL systems within the temperature range of 283.1–348.15 K was utilized. Furthermore, an outlier analysis was used to discover doubtful data points. Gained values of MSE & R^2 were 0.0000007 and 0.993, 0.0000002 and 0.998, 0.0000004 and 0.996 and 0.0000006 and 0.994 for the ICA-ANN, TLBO-ANN, PSO-ANN and GA-ANN, respectively. Results demonstrated that the experimental data and predicted values of the TLBO-ANN model for such target are wholly matched.

Keywords Surface tension · Ionic liquid · Artificial neural network · Genetic algorithm · Teaching–learning-based optimization · Imperialist competitive algorithm · Particle swarm optimization

✉ Reza Daneshfar
reza_daneshfar@ut.ac.ir

✉ Maryam Naseri
naaseri1375@gmail.com

[1] Universitas Kristen Petra, Surabaya, Indonesia

[2] Department of Petroleum Engineering, Ahwaz Faculty of Petroleum Engineering, Petroleum University of Technology (PUT), Ahwaz, Iran

[3] Department of Chemical Engineering, Faculty of Engineering, Golestan University, Aliabad Katoul, Iran

Published online: 11 April 2021

List of symbols

IL	Ionic liquid
ANN	Artificial neural network
MRE	Mean relative error
ICA	Imperialist competitive algorithm
R^2	Coefficient of determination
STD	Standard deviation
MLP	Multi-layer perceptron
SVM	Support vector machine
ST	Surface tension
MSE	Mean squared error
BP	Back-propagation
PSO	Particle swarm optimization
EC	Evolutionary computation
ARD	Average relative deviation
GA	Genetic algorithm
TLBO	Teaching–learning-based optimization
RMSE	Root-mean-squared error
DT	Decision tree
FS	Fuzzy system
GEP	Gene expression programming
RBF	Radial basis function
BP	Backpropagation
AI	Artificial intelligence
r	Relevancy factor

1 Introduction

In recent years, the use of new chemicals such as nanoparticles, ionic liquids, and surfactants has opened a new window on research (Bakthavatchalam, 2020; Dehaghani & Daneshfar, 2019; Keykhosravi & Simjoo, 2018, 2019, 2020). Among these materials, ionic liquid has been introduced in various sciences such as chemical engineering and petroleum engineering and has received much attention (Harada et al., 2020; Liu, 2016). In a simple word, small organic or inorganic anions and almost large organic cations make up a new set of ionic organic salts whose melting points are below or near the ambient temperature, known as ionic liquids (ILs) (Baghban, 2015). The exceptional applicability of ILs in comparison to more conventional compounds has drawn great attention in both industry and academia. This is mainly due to their high ionic conductivity, very low volatility, high stability (thermal and electronic), good solubility, and a wide liquid temperature range (Vega, 2010). Of course, a knowledge of thermophysical and physicochemical attributes of the accompanying ILs is crucial to design an effective process (Gharagheizi, 2013). Especially, precise information about the ST of these fluids and their mixtures is indispensable in exploitation and designing modern industrial processes such as extraction, absorption, and also distillation involving IL (Carvalho, 2008; Oliveira, 2012). In recent years, many researchers have entered the field of laboratory studies of ionic liquids (Asl, 2020; Mosallanejad et al., 2018; Shaahmadi et al., 2018; Tajikmansori et al., 2020), and a number of them have measured the surface tension of compounds containing these substances (Oz,

2020; Shojaeian, 2019). Clearly, the experimental measurement cannot take the properties of each possible IL and its mixture with other compounds because there are infinite numbers of conceivable systems. Besides, empirical measurements usually involve expensive, time-consuming procedures and the measurements might suffer from non-negligible uncertainties (Gharagheizi, 2013). Thus, developing a reliable method for estimating the diverse properties of these kinds of systems will be extremely attractive (Baghban, 2015). In the literature, meticulous articles on the estimation methods of pure compounds ST have been previously offered (Dehaghani, 2019; Gharagheizi, 2013). A review of the ST approximation of ILs has been collected by (Tariq, 2012) and (Gharagheizi et al., 2012). Briefly, they demonstrated associated deficiencies of the methods utilized for modeling of ST of ILs and their accompanying mixtures. They represented that these methods have their disadvantages. Also, this fact was shown that ST of ILs is an open field of research because modeling of such property is predicted by few models.

Gharagheizi and his colleagues (Gharagheizi et al., 2012) had employed a group-contribution method which is not occasionally beneficial in terms of simplicity and time as it requires a detailed understanding of the IL structures. Also, the specification of group parameters for different functional groups of IL structures has not been still available (Hezave, Lashkarbolooki, et al., 2012). Because of the restricted usage of such methods, the lack of an alternative method makes sense.

Recently, emerging artificial intelligence (AI) methods, including least square support vector machine (LSSVM) (Faghihi et al., 2019; Kardani, 2018; Kardani & Baghban, 2017; Nabipour, 2020), ANN (Daneshfar, 2020a; Kardani, 2019; Vanani et al., 2019), multivariate adaptive regression splines (MARS) (Choudhury et al., 2020), adaptive neuro-fuzzy inference system (ANFIS) (Daneshfar, 2020b; Daryasafar et al., 2019; Ghadiri, 2020), group method of data handling (GMDH) (Majumder et al., 2019), and firefly algorithm (De & Majumder, 2019) are accepted as an adequate approach especially in the development of a model for complex systems (Dehaghani, 2019). In this regard, these methods have been applied as efficient and viable tools in a great deal of research works over the past decades due to their simple implementation in multi-functional problems (Alrashed, 2018; Bagherzadeh, 2019; Bahrami, 2019; Karimipour, 2018, 2019; Moradikazerouni, 2019; Peng, 2020; Qu et al., 2020; Safaei, 2019; Wu, 2019; Zhu, 2019).

In the last decade, various studies have reported the successful use of intelligent methods to correlate the properties of ILs. Hezave et al. investigated systems containing ILs demonstrating appropriate predictability of ANNs for pure ILs' thermal conductivity (Hezave, Raeissi, et al., 2012), binary heat capacity (Lashkarbolooki et al., 2012), binary density (Lashkarbolooki et al., 2013), ternary bubble points (Hezave et al., 2013), ternary electrical conductivity (Hezave, Lashkarbolooki, et al., 2012), and ternary viscosity (Lashkarblooki, 2012).

Among these interesting and innovative methods, the attention of some researchers has been drawn to AI models in order to predict the different properties of pure (Deng et al., 2020; Lazzús, 2017; Low et al., 2020; Mulero et al., 2017; Wang et al., 2021), binary (Lashkarbolooki, 2017; Lashkarbolooki et al. 2012, 2013), and ternary (Hezave et al. 2013) systems containing IL.

In the last few years, various innovative methods have been used to predict the surface tension of pure ILs (Atashrouz et al. 2017; Lazzús, 2017). According to the latest study in literature, few works have predicted the surface tension of IL binary systems using various artificial intelligence methods which are described below (Atashrouz, 2017; Hashemkhani, 2015; Lashkarbolooki, 2017; Shojaeian & Asadizadeh, 2020; Soleimani, 2018).

In 2015, Hashemkhani et al. used SVM and LSSVM models coupled with coupled simulated annealing (CSA) and GA to predict the surface tension of binary mixtures containing 748 data and 31 different IL mixtures (Hashemkhani, 2015). They considered temperature, liquid ionic properties (including mole fraction, molecular weight and density), and non-ionic liquid properties (including boiling temperature and molecular weight) as input parameters of their models. They concluded that the CSA-LSSVM model has a better ability to predict target values compared to other models, which results in $R^2 = 0.987044$ and RMSE = 1.629 E-3. In 2017, Atashrouz and his colleagues used the GA-LSSVM, GA-SVM, and group method data handling type polynomial neural network (GMDH-PNN) models to estimate the surface tension of binary mixtures containing ionic liquid (Atashrouz, 2017). They analyzed 573 data containing 32 different mixtures. The input data of their models were temperature and properties of ionic and non-ionic liquids (including mole fraction and density). They concluded that the two models GA-LSSVM and GA-SVM have a higher ability to predict laboratory values of surface tension compared to the GMDH-PNN model. Although their proposed models have a high accuracy in predicting the results (maximum value of R^2 equal to 0.9989), the number of input data as well as the number of input parameters to their models are less compared to other similar works, and it is possible that if they took into account more data, the accuracy of their models would be less. In 2017, Lashkarbolooki used the artificial neural network to provide a model for predicting the surface tension values of binary mixtures containing ionic liquid. His model was made up of 836 input data consisting of 32 different mixtures, and the input parameters to his model included temperature and properties of the ionic and non-ionic liquid (including melting temperature, mole fraction, and molecular weight). This model was able to predict the output data with $R^2 = 0.9948$ and MSE = 6.67 E-7. In 2018, Soleimani and his colleagues used a model based on an artificial neural network to predict the surface tension of mixtures containing ionic liquid (Soleimani, 2018). They used 748 data and were able to accurately predict the output parameter by considering the input parameters of their model including temperature, ionic liquid properties (mole fraction and molecular weight), and non-ionic liquid properties (boiling temperature and molecular weight). According to statistical analysis, their model was able to predict surface tension with $R^2 = 0.9995726$ and AARD% = 0.44%. By examining the input parameters and trying to predict an accurate model in 2020, Shojaeian and Asadizadeh showed that the ANN model has a good ability to predict the surface tension of binary mixtures containing ionic liquid (Shojaeian & Asadizadeh, 2020). The best model they proposed was a model with root-mean-square error (RMSE) equal to 7.88×10^{-3}.

In this article, the effect of different parameters on the ST of various binary mixtures of ILs has been studied using a new modeling approach according to ANN coupled by four powerful optimization algorithms, namely TLBO, PSO, GA, and ICA. To this end, a big dataset of binary ST of IL systems is collected from the literature. Then, for estimating the accurate ST, models are developed based on effective inputs such as the operational temperature (T) and ILs'/non-ILs' specifications. Next, statistical analysis was used for evaluating the efficiency of the recommended models. Then, we use William's analysis to evaluate the accuracy of the actual results from which the model is made. Finally, a sensitivity analysis was used to determine the most important parameters affecting the output.

2 Materials and methods

This section provides a complete description of the models and algorithms used to predict the target parameter.

2.1 ANN

As a computational intelligence model, ANN can learn from experience, improve its performance, and adapt to environmental fluctuations (Mohanraj et al., 2015). ANNs are systems dispersed in parallel comprised of simple components called neurons, as operating elements, which are arrayed in layer(s) and interrelated by connections. Two widespread ANNs are MLP and radial basis function (RBF) networks. A representative MLP neural structure contains three groups of layers (input, hidden, and output). Each layer contains several neurons and the number of neurons in the hidden layer should be optimized via optimization methods. The MLP structure connections deal with the variables of equivalent problems; the training procedure is performed by way of interconnections construction. It is noteworthy that these interconnections must be established optimally (by adopted optimization techniques) to build up an effective MLP structure (Baghban et al., 2015).

On the other hand, RBF-ANNs are more facile in designing compared to MLP-ANNs while they are also capable of responding quite properly to patterns that were not applied in the training procedure (Yao, 2004). As a class of feedforward neural networks, the design of RBF-ANNs depends on the iterative estimation of localized basis function networks. Due to a simpler structure and a more quick training process, RBF-ANN is a favorable alternative to the MLP-ANN (Girosi & Poggio, 1990). RBF-ANN structure also includes a hidden layer, input layer, and output layer. RBF is used for every node in the hidden layer and it comprises this nonlinear activation function as a network neuron. The precise shape, the distance scale, and the center of the radial function are the model parameters. The whole parameters are adjusted if it is linear. According to the linear optimization approach, the RBF-ANN can provide an inclusive optimum solution to the adaptable weights in the minimal MSE. The output of the RBF-ANN is presented as follows (for an input pattern x) (Du & Swamy, 2006):

$$y_i(x) = \sum_{k=1}^{h} W_{ki} \varnothing\left(\|x - x_k\|\right) \tag{1}$$

x_k is the archetype of the center of the *k_th* hidden unit,W_{ki} is the connection weight between the *k_th* hidden unit and the *i_th* output unit, and ‖‖ symbolizes Euclidean norm. The Gaussian function that is utilized here is the RBF (φ). The Gaussian is a representative radial function that is incorporated in Eq. (2) (in the event of a scalar input) (Du & Swamy, 2006):

$$h(x) = \exp\left(-\frac{(x-c)^2}{r^2}\right) \tag{2}$$

The radius and center are the parameters of Gaussian RBF that have been denoted by r and c, respectively. Getting away from the center makes a Gaussian RBF undergo monotonic reductions. Contrarily, distancing from the center (in the event of scalar input) causes a monotonic rise in a multi-quadric RBF as expressed in Eq. (3) (Bemani et al., 2019):

$$h(x) = \frac{\sqrt{r^2 + (x - c)^2}}{r} \tag{3}$$

Gaussian-like RBFs are local with further common uses than multi-quadric type RBFs which have a universal response. Gaussian-like RBFs are also of more biological plausibility due to their finite responses (Park & Sandberg, 1991; Schilling et al. 2001).

2.2 TLBO

In a relatively recent study, Rao et al. (Rao et al., 2012) offered the TLBO algorithm (Yildiz, 2013). A population that consists mostly of ''learners" prompts enhancements to advance swiftly toward an optimal solution in this algorithm. Our research covers a population of 250 preliminary "learners" cooperating with a limited few numbers of ''teachers" via two activities: 1) the teacher stage, which involves enhancement resulting from the current science of the teacher(s), and then 2) the learner stage, which involves enhancement obtained from interplay with the increasingly acquired knowledge from inside the learner population.

Developing the general performance of the learner population according to the mean result of the teacher's current knowledge originates from the teacher stage of the class from whatever value to its level based on its capacity (Nazari, 2020). If the quality of the teacher's solutions is shown by T_i and the average performance of the learners' solutions in whatever special iteration i is denoted by M_i, then T_i is used to elevate the value of M_i, i.e., prompting alterations that cause M_i to proceed toward an amended/enhanced average performance,M_{new}, closer to T_i. According to Murty et al. (Črepinšek et al., 2012), Eq. (4) instigates the modifications done as part of the teacher phase:

$$Difference\_Mean_i = r_i\left(M_{new} - T_F M_i\right) \tag{4}$$

In the above equation:T_F is the teaching factor, which can modify the average value of the learners under adjustment. A uniform random number in [0, 1] interval is chosen and denoted by r_i. T_F is chosen at random (with equivalent likelihood) to obtain values of either 1 or 2 (i.e., integer or rounded values) based on the association presented in Eq. (5) (Rao et al., 2012):

$$T_F = round[1 + rand(0, 1)(2 - 1)] \tag{5}$$

Using Eq. (6), a learner's solution in iteration i is changed from its solution in the prior iteration (i-1) (Rao et al. 2012):

$$X_i = X_{i-1} + Difference\_Mean_i \tag{6}$$

The learner phase concentrates on the improvement of the learners' solutions quality via interplay amongst the learner population throughout every iteration of this algorithm. Adjustment of a learner's solution is done toward solutions of those learners in the population who possess greater performance solutions. For two separate learners X_j and X_k, where solutions $j \neq k$, during each iteration i of the TLBO, Eqs. (7) and (8) are proposed by Rao et al. (Rao et al. 2012) to instigate learner modifications:

$$\text{If} f\left(X_j\right) < f\left(X_k\right) \text{then} X_{,i} = X_{i-1} + r_i\left(X_j - X_k\right) \tag{7}$$

or,

$$\text{If} f\left(X_j\right) > f\left(X_k\right) \text{then} X_{,i} = X_{i-1} + r_i\left(X_k - X_j\right) \tag{8}$$

The X_i values are obtained with Eqs. (7) or (8) are solely acceptable in case the values create a function (e.g., $f(X_j)$ or $f(X_k)$), which is enhanced from prior iteration $i - 1$.

The simplicity of the modifications included in Eqs. (4)–(8) facilitates the coding and implementation of TLBO.

2.3 GA

The preliminary step is to form the primary population to initiate the GA-related process. The next stage is to assess every individual by a suitable statistical fitness function followed by examining every individual's compatibility. The alleged ''Global Best Satisfactory'' individual has been created when the resulting error is permissible. The algorithm has to be ended with extracting the parameters; otherwise, the next stage is to select the weaker individuals for removal. Then, randomized cross-over and mutation processes are purposively performed to produce a novel population whose parameters lead to lowering the level of error, which is feasible by shifting to the stage of the ''Evaluation Fitness'' (Jefferys, 1993; Romero & Carter, 2001).

2.4 PSO

This plan begins with initializing the prime population with the dedication of locations and velocities randomly. It is followed by the fitness of every particle, which is done by making use of a statistical function. The criteria have to be abandoned and the assumed parameters have been created when the best particle's fitness rate meets the stopping criteria. However, failure to reach this rate can be redressed by updating the speeds and locations of particles under specific conditions. In this case, the first stage is to update the linked parameters of the universal best, in case the particle fitness is higher than that of the global best, and then to update the elements relating to the particle best, if the particle fitness is higher than the that of particle best. In the end, the next particles need to be reevaluated by a shift toward the second stage (Zendehboudi, 2012, 2014).

2.5 ICA

This algorithm is based upon forming several empires and displacing some colonies between empires, followed by questioning the charge of a colony for an empire. In the case of a high colony cost, the roles of imperialist and colony need to be altered. In the subsequent phase, the charge of total empires is calculated. The weakest colony of the weakest empire has to be assigned to the empire with the uppermost level of potential, as the succeeding stage. After that, an empire with no colonies has to be removed. In the subsequent level, the ending situations are examined to find the level of gratification to halt the algorithm (Ahmadi, 2013; Zendehboudi, 2013).

2.6 Prediction of ST values by the TLBO-ANN model

The presently introduced hybrid model applies a customary ANN and integrates it into TLBO to network training. The clarity of the ANN technique can be improved by its hybridization with TLBO, which can be advantageous both theoretically and practically.

The development of the hybrid TLBO-ANN model involves seven forthright stages:

(1) Organization and introduction of the dataset for analysis.
(2) Normalization of the data such that ANN would be able to process the data, which is done using Eq. (9) (Chu, 2017):

$$X_N = 2\frac{X - \min(X)}{\max(X) - \min(X)} - 1 \tag{9}$$

In which for a given data point, X_N denotes the normalized value of variable X.
(3) Preparation of testing and training data subgroups from the normalized data points. The training set comprised 561 data sets chosen at random which is utilized in the proposed model. For training the neural network, this training set will be used. About 25% of the collected data (187 data set) comprise the testing subgroup. Upon processing the training subgroup by the ANN, the accurate status of the constructed model is evaluated by testing the subgroup.
(4) Using a three-layer feedforward ANN to process the training set: this ANN structure was detected to have the highest effectiveness for this problem, which includes an output layer, an input layer, and a hidden (latent). In this process, only one hidden layer (including 20 neurons) is used. Activation (or transfer) functions process the data that is to be transferred between the ANN layers. Some options exist for the transfer functions, viz. nonlinear, sigmoidal, and piecewise linear functions which are more common (Ahmed & Sarma, 2007; Dorofki, 2012). For the introduced model, tansig (hyperbolic tangent) activation function is used between input and first hidden layer, logsig (log-sigmoid) activation function is used between the first hidden layer and second hidden layer, and purelin (linear) is used as the activation function between output and second hidden layer.
(5) In this step, the TLBO algorithm is used for network training. This is the combined stage and amendment to the customary ANN method, which uses the BP (back-propagation) algorithm for network training for almost 30 years (Rumelhart et al., 1986) and is still an acceptable standard (Nielsen & Neural networks & deep learning. Vol., 2018). The TLBO helps improve the efficacy and clarity of network training.
(6) Testing a subgroup of data points from step 3 (that do not contribute to steps 4 and 5) helps to assess the trained network's performance power.
(7) Analysis and presentation of the findings, namely performing statistical examination using other correlations and algorithms, repeating the algorithm run to confirm duplicability, and proving the relative influences of the dependent variables on the outcomes by the sensitivity examination.

(1) Organization and introduction of the dataset for analysis.

2.7 Estimation of ST values by the GA-ANN model

In the GA-ANN model, after developing the ANN, GA was utilized to optimize the weights and biases for predicting ST. According to Nguyen et al. (Nguyen et al., 2019), regression problems could be solved by at most two hidden layers of the ANN model. Accordingly, the procedure of "Trial and Error" was implemented using one and two hidden layers. Using the scale method of min–max, the overfitting of the initial ANN model was avoided by fixing the range in the interval [− 1, 1]. The performance of the GA optimization was evaluated based on the values of the RMSE and there were 1000 search iterations to gain the optimal weights and biases corresponding to the lowest RSME. The GA-ANN model was trained using the BP algorithm.

2.8 Estimation of ST values by the PSO-ANN model

Here, the ST values were predicted based on PSO-ANN, in which the weights and biases optimization phase were conducted using the PSO algorithm. The same developing techniques as in the GA-ANN model, such as scaling and back-propagation algorithm, were used in the PSO-ANN. The case with the lowest RMSE was determined as the best PSO-ANN model.

2.9 Estimation of ST values by the ICA-ANN model

The ST values were also predicted by the ICA-ANN model. Like the other three previous ANN optimization algorithms, the ICA algorithm was utilized to optimize the ANN elements. Then, the colonies, i.e., biases and weights, were globally searched by the imperialists' competition. As expected, the best ICA-ANN model had the lowest RMSE. Although the PSO-ANN, GA-ANN, and the ICA-ANN structures are similar, their biases and weights are different. It is noteworthy that the development techniques for these three models are also the same, i.e., the BP algorithm and the min–max scale [− 1, 1].

3 Case study

This section provides explanations about the steps of collecting laboratory data, how to use and analyze these data in order to model output values.

3.1 Data acquisition

For achieving the desired goals, a set of 748 experimental data of binary ST mixtures were collected from literature (Ahosseini, 2009; Dong, 2007; Dong, et al., 2006; Geppert-Rybczyńska, 2013; Harris et al., 2006; Jiang, 2013; Kermanpour & Niakan, 2012; Machida, 2010; Mallard & Linstrom, 2000; Rilo, 2009, 2012; Seki, 2012; Troncoso, 2006; Vakili-Nezhaad, 2012; Wandschneider et al. 2008; Wang, 2011a, 2011b; Wei, 2010). Independent input variables must be selected for models in the next step. Accordingly, input parameters were the operational temperature (T), ILs' specifications (including the molecular weight of the components (Mw_{IL}), the density of the

components (ρ_{IL}) and the component compositions (x_{IL})), and non-ILs' specifications (including molecular weight ($Mw_{non\text{-}IL}$) and boiling point ($Tb_{non\text{-}IL}$)) and the target variable is the ST of IL containing binary mixtures. The ST was then estimated using a dataset that was randomly divided into two distinct data collection, i.e., testing dataset and training dataset with the proportion of 25% and 75% of total data points, respectively. In order to model the desired process, we used MATLAB toolbox ANN code and coupled it with optimization codes to determine optimized weight and bias values. As an operational note, the performance of the proposed models has been evaluated using test data points which must not be employed at the training stage.

3.2 Implementation and analyses

This study has been aimed at estimating ST for binary mixtures involving ILs via the development of four computational models, including PSO-ANN, GA-ANN, TLBO-ANN, and ICA-ANN applied to the operational temperature (T) and ILs' & non-ILs' specifications. Based on the theoretical background, specific optimization algorithms (PSO, GA, TLBO, and ICA) should be used for optimizing the bias and weight terms of the ANN. After optimization, accuracy and capability of the four models would be examined through statistical analyses, including average relative deviation (ARD), root-mean-square error (RMSE), R-squared (R^2), standard deviation (STD), and mean squared error (MSE) as described below (Ahmadi, 2020):

$$\mathrm{MSE} = \frac{1}{N}\sum_{i=1}^{N}\left(\alpha_{\exp} - \alpha_{cal}\right)^2 \tag{10}$$

$$\mathrm{ARD}(\%) = \frac{100}{N}\sum_{i=1}^{N}\frac{\alpha_{\exp} - \alpha_{cal}}{\alpha_{\exp}} \tag{11}$$

$$\mathrm{STD}_{\mathrm{error}} = \left(\frac{1}{N-1}\sum_{i=1}^{N}\left(\mathrm{error} - \overline{\mathrm{error}}\right)^2\right)^2 \tag{12}$$

$$R^2 = \frac{\left[\sum_{i=1}^{N}\left(\alpha_{\exp} - \overline{\alpha_{\exp}}\right)\left(\alpha_{cal} - \overline{\alpha_{cal}}\right)\right]^2}{\left[\sum_{i=1}^{N}\left(\alpha_{\exp} - \overline{\alpha_{\exp}}\right)\sum_{i=1}^{N}\left(\alpha_{cal} - \overline{\alpha_{cal}}\right)\right]} \tag{13}$$

$$\mathrm{RMSE} = \sqrt{\left(\frac{1}{N}\sum_{i=1}^{N}\left(\alpha_{\exp} - \alpha_{cal}\right)^2\right)} \tag{14}$$

where the term N stands for the number of total data points, and also $\alpha_{\exp}$ and α_{cal} represent actual and estimated data points in the above equations.

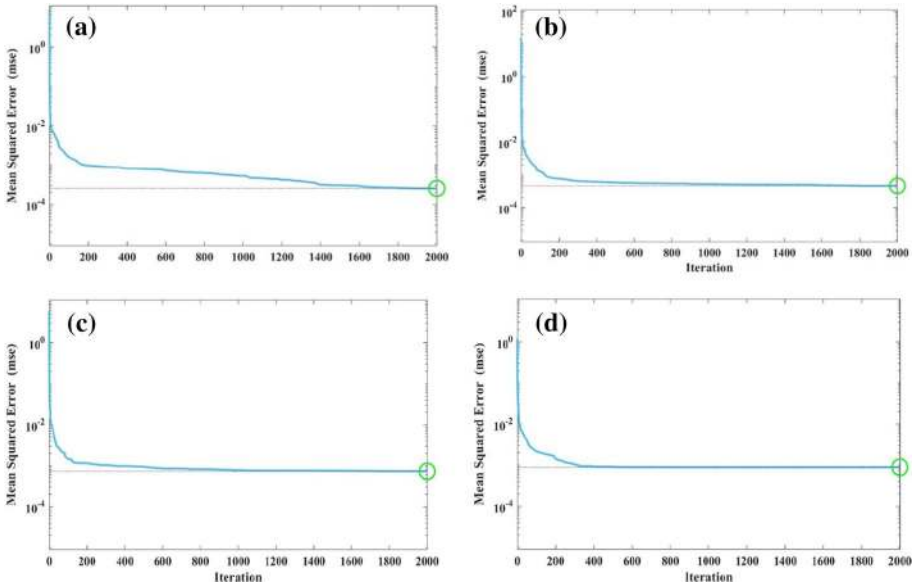

Fig. 1 Performance (MSE) plot of the ANN models for estimating ST by **a** TLBO-ANN **b** PSO-ANN **c** GA-ANN and **d** ICA-ANN

Table 1 Details of the proposed models

Model	Parameter	Value/comment
ICA	$N_{country}$	85
	N_{imp}	10
	β	1.7
	γ	0.2
	ξ	0.2
	Revolution rate	0.4
PSO	Swarm size	85
	C1	2
	C2	2
GA	Population	85
	Generation	2000
TLBO	Population	85
	Iteration	2000
ANN structure	Hidden neuron	20
	Hidden layer	1
	Transfer function	Sigmoid

4 Results and discussion

The ANN optimization was accomplished using PSO, GA, TLBO, and ICA algorithms. The performances of the proposed models are compared in Fig. 1 which indicates the mean square of errors for estimated and actual data points versus the number of

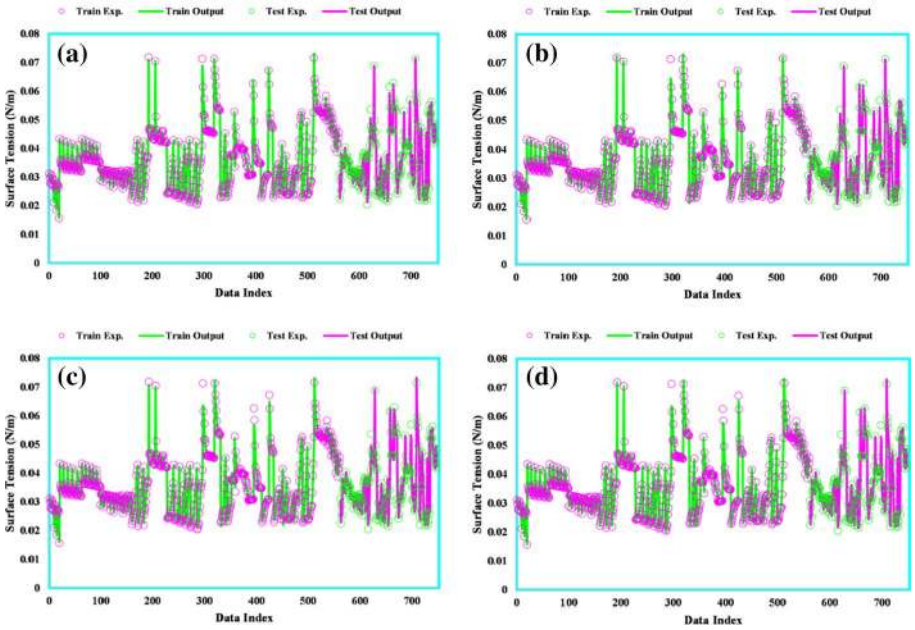

Fig. 2 Actual versus estimated ST by the proposed models at training and testing stages: **a** TLBO-ANN **b** PSO-ANN **c** GA- ANN and **d** ICA-ANN

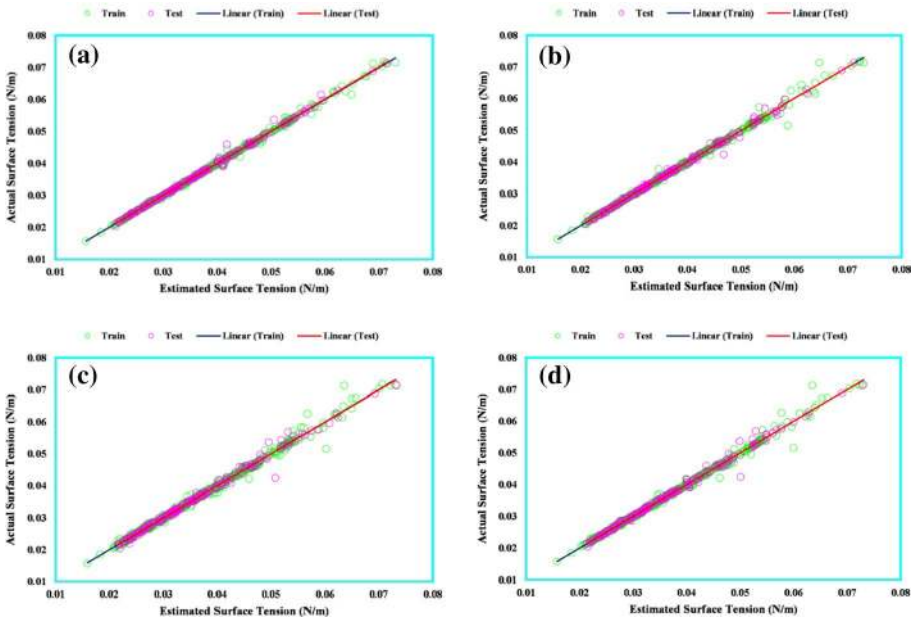

Fig. 3 Regression plots estimation of the ST using the proposed models at training and testing stages: **a** TLBO-ANN **b** PSO-ANN **c** GA- ANN and **d** ICA-ANN

the corresponding iteration. This Figure shows that the number of iterations which is required to minimize MSE is 2000, 1000, 1000, and 400 for the TLBO-ANN, PSO-ANN, GA- ANN, and ICA-ANN, respectively. Table 1 also provides more information about these four models. This table contains the values of utilized parameters in the different proposing algorithms that are set based on our expertise.

Figure 2 graphically explains the estimated and actual ST of mixtures for both testing and training stages. According to this Figure, it is clear that all models have a relatively good ability to predict experimental values at the training and testing stages because, as can be seen, the values of the laboratory and the model are very close to each other. According to this analysis, apparently, all models have a good ability to predict laboratory values. In order to clarify the issue and determine the best model, we will continue with other analyzes.

Figure 3 demonstrates the regression between actual values and results achieved from the proposed models. Real values have a relationship with model outputs as indicated by the R^2 value. This relationship would be exactly linear if R^2 is equal to unity. Figures representing the regression obviously show that the TLBO-ANN model has the most accurate fitting. Diagrams of ST of binary mixtures containing ethanol & [BMIM][L-lactate], methanol & [BMIM][L-lactate] and dimethyl sulfoxide & [EMIM][TF2N] as a function of IL concentration and temperature are presented in Figs. 4, 5 and 6.

As a consequence, different statistical analyses, including MSE, RMSE, STD, ARD, and R^2, were employed to investigate the models' capability. Figure 7 represents relative

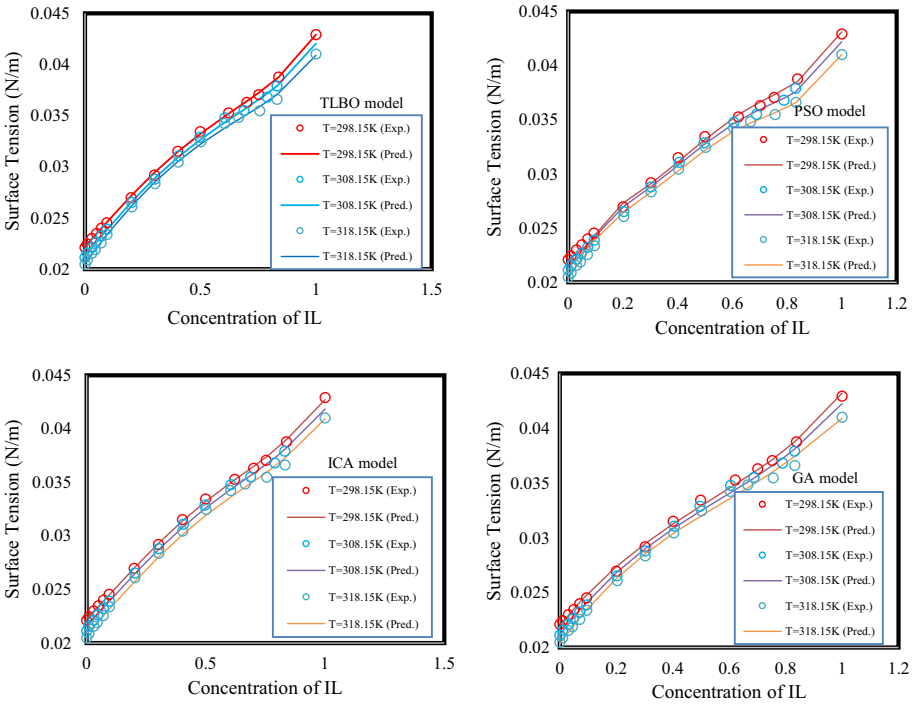

Fig. 4 Diagram of ST of binary mixture ethanol and [BMIM][L-lactate] as a function of temperature and concentration of IL component

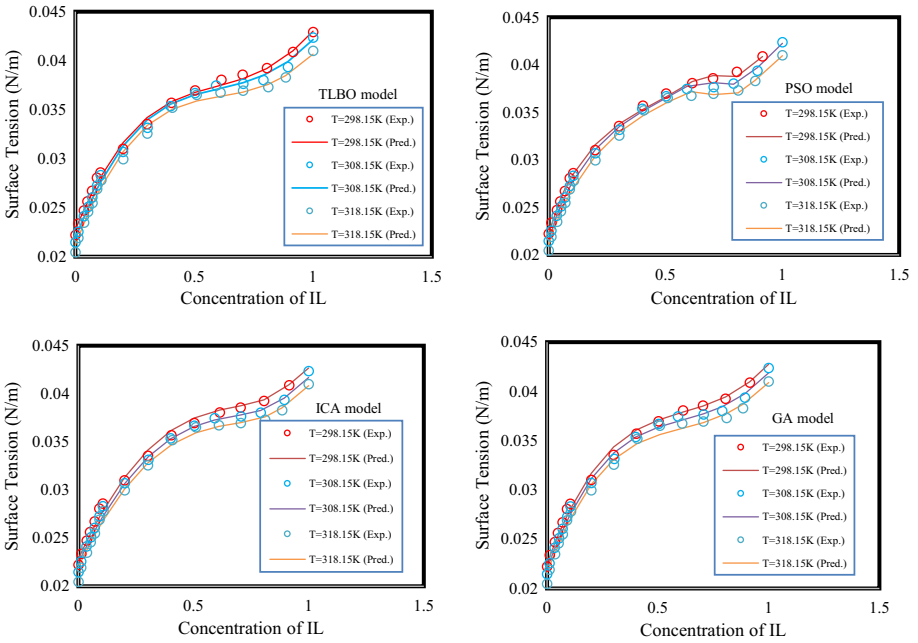

Fig. 5 Diagram of ST of binary mixture methanol and [BMIM][L-lactate] as a function of temperature and concentration of IL component

deviations of estimated and actual ST mixtures of models in percentage. Additionally, Table 2 provides the values of RMSE, MSE, R^2, ARD, and STD at training and testing phases, respectively. Also, Fig. 8 (known as William's plot) demonstrates the leverage analysis of ST estimation for detecting outliers in the dataset which have higher hat values in comparison with warning leverage hat value as well as standardized remaining values out of the acceptable range of + 3 to − 3.

4.1 Sensitivity analysis

ANN models relate the input to the output and sensitivity analysis examines how variations in the input can influence the output. The present study has chosen TLBO-ANN as the best model structure. Chen et al. (2014) introduced the relevancy factor (r) equation to find the most effective input as well as the effect of each input on the output values (Chen, 2014). The value of r ranges from −1 to + 1. Observing input and output with high absolute values of r shows a higher impact of input on the output. Negative and positive coefficients are, respectively, obtained when the increment of input causes an increase or a decrease in the output. Figure 9 represents a direct relationship between ST, IL's mole fraction (x_{IL}) and boiling point of non-ILs (Tb_{non-IL}). It also indicates an inverse dependency between ST and the operational temperature (T), the density of IL ($_{IL}$) and molecular weights of IL (Mw_{IL})/ non-IL (Mw_{non-IL}) components. Moreover, it was found that the IL mole fraction (x_{IL}) has the most important effect on ST of the mixtures with $r = 0.1$, while the molecular weight of non-ILs (Mw_{non-IL}) has the minimum effect on that with$r = -0.55$.

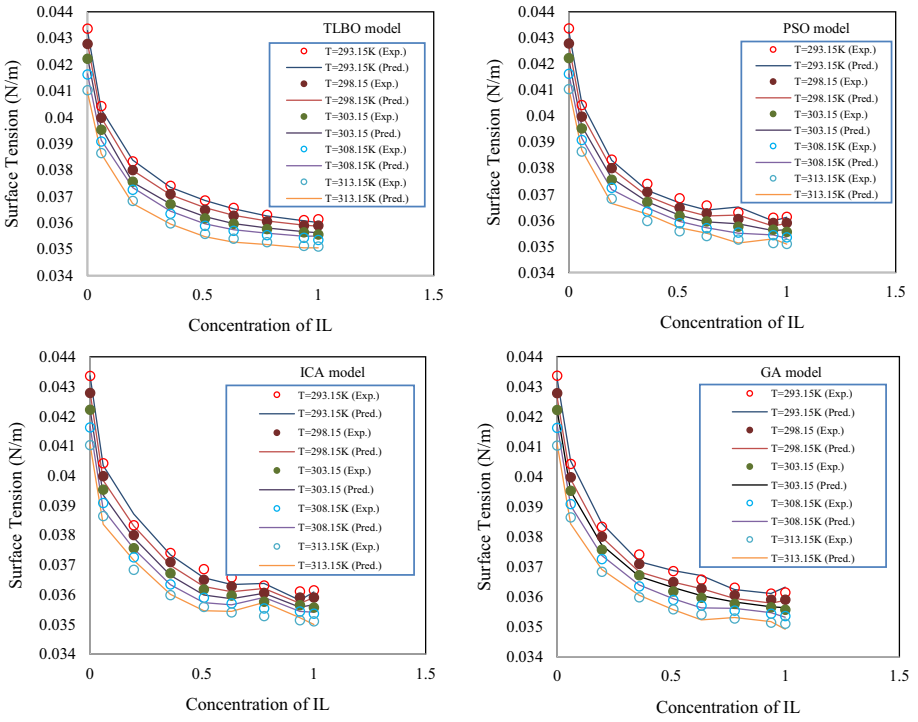

Fig. 6 Diagram of ST of binary mixture dimethyl sulfoxide and [EMIM][TF2N] as a function of temperature and concentration of IL component

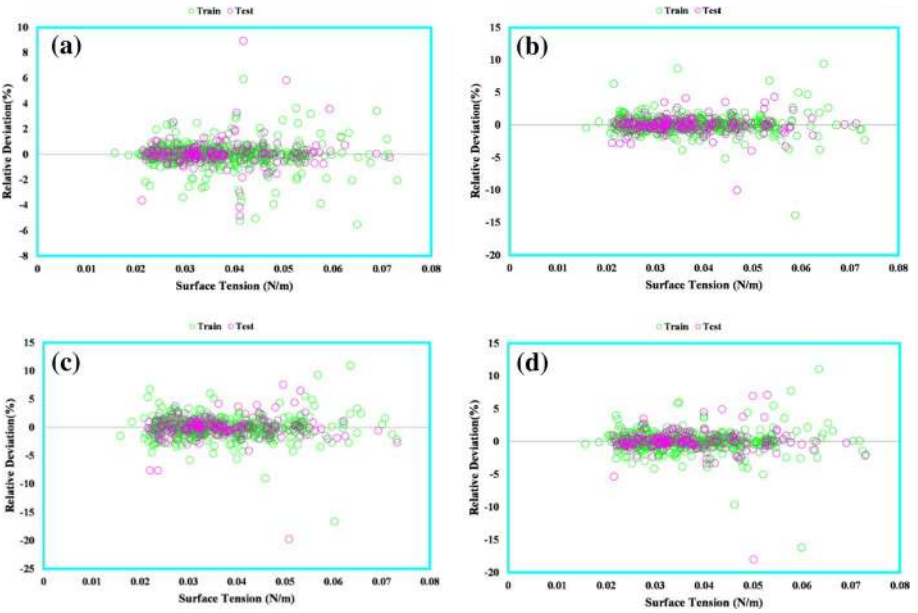

Fig. 7 The percentage of relative deviation between the actual and estimated density using: **a** TLBO-ANN **b** PSO-ANN **c** GA- ANN and **d** ICA-ANN

Table 2 Evaluating the performance of proposed models using statistical analysis

Model	Data Set	R^2	MRE (%)	MSE	RMSE	STD
TLBO-ANN	Train	0.998	0.520	0.0000002	0.0004	0.0004
	Test	0.997	0.614	0.0000003	0.0005	0.0005
	Total	0.998	0.543	0.0000002	0.0005	0.0004
PSO-ANN	Train	0.996	0.674	0.0000004	0.0006	0.0006
	Test	0.997	0.803	0.0000003	0.0006	0.0005
	Total	0.996	0.706	0.0000004	0.0006	0.0005
GA-ANN	Train	0.995	0.812	0.0000005	0.0007	0.0007
	Test	0.993	0.971	0.0000007	0.0008	0.0008
	Total	0.994	0.852	0.0000006	0.0008	0.0007
ICA-ANN	Train	0.994	1.118	0.0000006	0.0008	0.0007
	Test	0.992	1.245	0.0000009	0.0009	0.0008
	Total	0.993	1.150	0.0000007	0.0009	0.0007

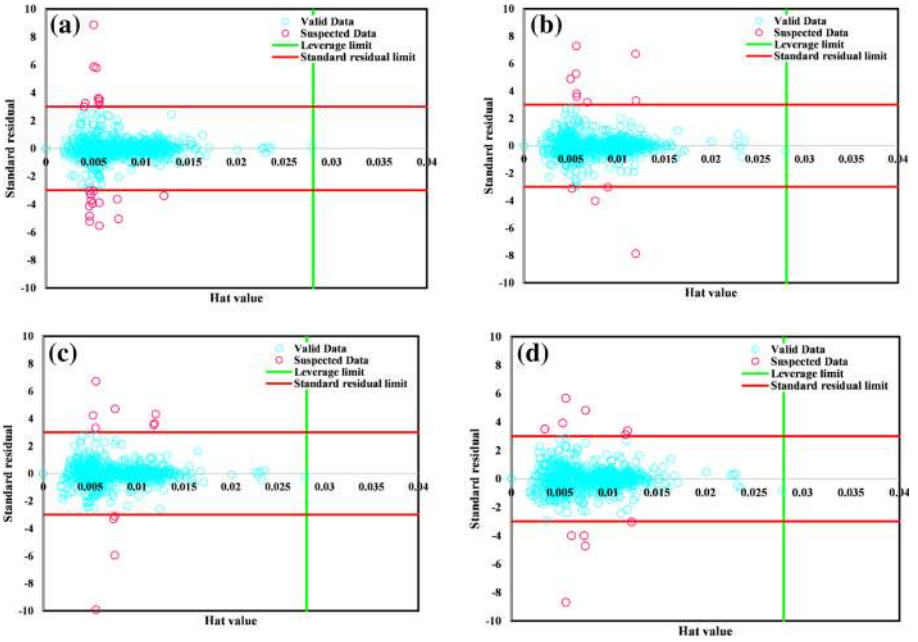

Fig. 8 William's plots for the estimation of ST by **a** TLBO-ANN **b** PSO-ANN **c** GA- ANN and **d** ICA-ANN

5 Conclusion

The present paper has applied an ANN model with four optimization algorithms (PSO, GA, TLBO, and ICA) for ST prediction in binary mixtures involving 31 different ILs according to the operational temperature, and ILs' & non-ILs' specifications. The proposed ANN model employed 748 data points collected from different literature resources as the

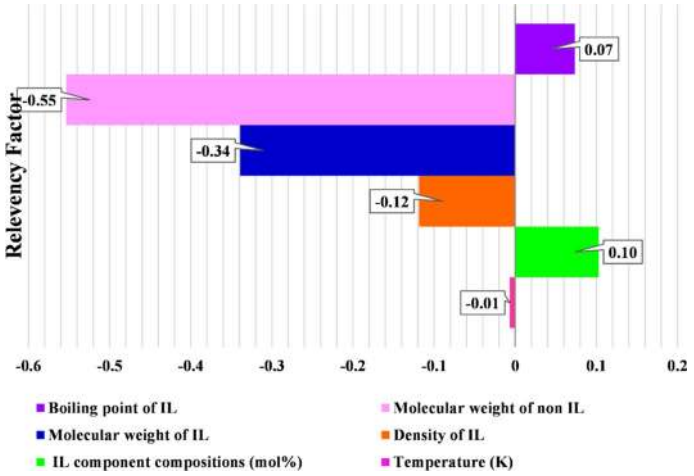

Fig. 9 Sensitivity analysis of the TLBO-ANN model to find out the effect of inputs on ST

training and testing sets. Statistical analyses indicated that the TLBO-ANN was the most accurate among the proposed models as confirmed by the leverage mathematical approach. Based on statistical analysis, this model has the ability to predict laboratory values with $R^2 = 0.998$, MSE = 0.0000002, and STD = 0.0004. Sensitivity analysis was then performed illustrating the IL's mole fraction and non-IL's molecular weight as the most effective and the least effective factor on ST, respectively. Furthermore, this easy-to-apply model would largely help chemical and petroleum engineers to estimate the ST of ILs and their relevant mixtures.

References

Ahmadi, M. A., et al. (2013). Evolving artificial neural network and imperialist competitive algorithm for prediction oil flow rate of the reservoir. *Applied Soft Computing, 13*(2), 1085–1098.

Ahmadi, M. H., et al. (2020). Evolving connectionist approaches to compute thermal conductivity of TiO2/water nanofluid. *Physica A: Statistical Mechanics and its Applications, 540*, 122489.

Ahmed, J. A., & Sarma, A. K. (2007). Artificial neural network model for synthetic streamflow generation. *Water Resources Management, 21*(6), 1015–1029.

Ahosseini, A., et al. (2009). Phase equilibrium, volumetric, and interfacial properties of the ionic liquid, 1-hexyl-3-methylimidazolium bis (trifluoromethylsulfonyl) amide and 1-octene. *Journal of Chemical & Engineering Data, 55*(4), 1611–1617.

Alrashed, A. A., et al. (2018). Effects on thermophysical properties of carbon based nanofluids: experimental data, modelling using regression, ANFIS and ANN. *International Journal of Heat and Mass Transfer, 125*, 920–932.

Asl, H. F., et al. (2020). Experimental investigation into l-Arg and l-Cys eco-friendly surfactants in enhanced oil recovery by considering IFT reduction and wettability alteration. *Petroleum Science, 17*(1), 105–117.

Atashrouz, S., et al. (2017). Implementation of soft computing approaches for prediction of physicochemical properties of ionic liquid mixtures. *Korean Journal of Chemical Engineering, 34*(2), 425–439.

Atashrouz, S., Mirshekar, H., & Mohaddespour, A. (2017). A robust modeling approach to predict the surface tension of ionic liquids. *Journal of Molecular Liquids, 236*, 344–357.

Baghban, A., et al. (2015). Phase equilibrium modeling of semi-clathrate hydrates of seven commonly gases in the presence of TBAB ionic liquid promoter based on a low parameter connectionist technique. *The Journal of Supercritical Fluids, 101*, 184–192.

Baghban, A., Ahmadi, M. A., & Shahraki, B. H. (2015). Prediction carbon dioxide solubility in presence of various ionic liquids using computational intelligence approaches. *The Journal of supercritical fluids, 98*, 50–64.

Bagherzadeh, S. A., et al. (2019). A novel sensitivity analysis model of EANN for F-MWCNTs–Fe3O4/EG nanofluid thermal conductivity: Outputs predicted analytically instead of numerically to more accuracy and less costs. *Physica A: Statistical Mechanics and Its Applications, 521*, 406–415.

Bahrami, M., et al. (2019). Develop 24 dissimilar ANNs by suitable architectures & training algorithms via sensitivity analysis to better statistical presentation: Measure MSEs between targets & ANN for Fe–CuO/Eg–Water nanofluid. *Physica A: Statistical Mechanics and its Applications, 519*, 159–168.

Bakthavatchalam, B., et al. (2020). Comparative evaluation on the thermal properties and stability of MWCNT nanofluid with conventional surfactants and ionic liquid. *Journal of Thermal Analysis and Calorimetry*. https://doi.org/10.1007/s10973-020-10374-x.

Bemani, A., et al. (2019). Applying ANN, ANFIS, and LSSVM models for estimation of acid solvent solubility in supercritical CO_2. arXiv preprint. http://www.techscience.com/cmc/v63n3/38869.

Carvalho, P. J., et al. (2008). Surface tensions for the 1-alkyl-3-methylimidazolium bis (trifluoromethylsulfonyl) imide ionic liquids. *Journal of Chemical & Engineering Data*. https://doi.org/10.1021/je800069z.

Chen, G., et al. (2014). The genetic algorithm based back propagation neural network for MMP prediction in CO2-EOR process. *Fuel, 126*, 202–212.

Choudhury, S., Saha, A. K., & Majumder, M. (2020). Optimal location selection for installation of surface water treatment plant by Gini coefficient-based analytical hierarchy process. *Environment, Development and Sustainability*, *22*, 4073–4099.

Chu, Z.-Q., et al. (2017). Modeling of wax deposition produced in the pipelines using PSO-ANFIS approach. *Petroleum Science and Technology, 35*(20), 1974–1981.

Črepinšek, M., Liu, S.-H., & Mernik, L. (2012). A note on teaching–learning-based optimization algorithm. *Information Sciences, 212*, 79–93.

Daneshfar, R., et al. (2020a). A neural computing strategy to estimate dew-point pressure of gas condensate reservoirs. *Petroleum Science and Technology*. https://doi.org/10.1080/10916466.2020.1780257.

Daneshfar, R., et al. (2020b). Estimating the heat capacity of non-Newtonian ionanofluid systems using ANN, ANFIS, and SGB tree algorithms. *Applied Sciences, 10*(18), 6432.

Daryasafar, A., Keykhosravi, A., & Shahbazi, K. (2019). Modeling CO2 wettability behavior at the interface of brine/CO2/mineral: Application to CO2 geo-sequestration. *Journal of Cleaner Production, 239*, 118101.

De, P., & Majumder, M. (2019). Allocation of energy in surface water treatment plants for maximum energy conservation. *Environment, Development and Sustainability*, *22*, 3347–3370.

Dehaghani, A. H. S., et al. (2019). Simulation study of the Gachsaran asphaltene behavior within the interface of oil/water emulsion: a case study. *Colloid and Interface Science Communications, 33*, 100202.

Dehaghani, A. H. S., & Daneshfar, R. (2019). How much would silica nanoparticles enhance the performance of low-salinity water flooding? *Petroleum Science, 16*(3), 591–605.

Deng, T., Liu, F.-H., & Jia, G.-Z. (2020). Prediction carbon dioxide solubility in ionic liquids based on deep learning. *Molecular Physics, 118*(6), e1652367.

Dong, Q., et al. (2006). Ionic Liquids Database (ILThermo). http://ilthermo.boulder.nist.gov/ILThermo/mainmenu.uix.

Dong, Q., et al. (2007). ILThermo: a free-access web database for thermodynamic properties of ionic liquids. *Journal of Chemical & Engineering Data, 52*(4), 1151–1159.

Dorofki, M., et al. (2012). Comparison of artificial neural network transfer functions abilities to simulate extreme runoff data. *International Proceedings of Chemical, Biological and Environmental Engineering, 33*, 39–44.

Du, K. L., & Swamy, M. N. (2006). *Neural networks in a softcomputing framework*. . Springer.

Faghihi, S., Keykhosravi, A., & Shahbazi, K. (2019). Modeling of kinetic adsorption of natural surfactants on sandstone minerals: Spotlight on accurate prediction and data evaluation. *Colloid and Interface Science Communications, 33*, 100208.

Geppert-Rybczyńska, M., et al. (2013). Thermodynamic surface properties of [BMIm][NTf2] or [EMIm][NTf2] binary mixtures with tetrahydrofuran, acetonitrile or dimethylsulfoxide. *The Journal of Chemical Thermodynamics, 62*, 104–110.

Ghadiri, M., et al. (2020). An insight into the estimation of relative humidity of air using artificial intelligence schemes. *Environment, Development and Sustainability,*. https://doi.org/10.1007/s10668-020-01053-w.

Gharagheizi, F., et al. (2013). Development of corresponding states model for estimation of the surface tension of chemical compounds. *AIChE Journal, 59*(2), 613–621.

Gharagheizi, F., Ilani-Kashkouli, P., & Mohammadi, A. H. (2012). Group contribution model for estimation of surface tension of ionic liquids. *Chemical engineering science, 78*, 204–208.

Girosi, F., & Poggio, T. (1990). Networks and the best approximation property. *Biological Cybernetics, 63*(3), 169–176.

Harada, M., Yamamoto, M., & Sakata, M. (2020). Temperature dependence on the size control of palladium nanoparticles by chemical reduction in nonionic surfactant/ionic liquid hybrid systems. *Journal of Molecular Liquids*. https://doi.org/10.1016/j.molliq.2020.113255.

Harris, K. R., Kanakubo, M., & Woolf, L. A. (2006). Temperature and pressure dependence of the viscosity of the ionic liquids 1-methyl-3-octylimidazolium hexafluorophosphate and 1-methyl-3-octylimidazolium tetrafluoroborate. *Journal of Chemical & Engineering Data, 51*(3), 1161–1167.

Hashemkhani, M., et al. (2015). Prediction of the binary surface tension of mixtures containing ionic liquids using support vector machine algorithms. *Journal of Molecular Liquids, 211*, 534–552.

Hezave, A. Z., Lashkarbolooki, M., & Raeissi, S. (2012). Using artificial neural network to predict the ternary electrical conductivity of ionic liquid systems. *Fluid Phase Equilibria, 314*, 128–133.

Hezave, A. Z., Lashkarbolooki, M., & Raeissi, S. (2013). Correlating bubble points of ternary systems involving nine solvents and two ionic liquids using artificial neural network. *Fluid Phase Equilibria, 352*, 34–41.

Hezave, A. Z., Raeissi, S., & Lashkarbolooki, M. (2012b). Estimation of thermal conductivity of ionic liquids using a perceptron neural network. *Industrial & Engineering Chemistry Research, 51*(29), 9886–9893.

Jefferys, E. (1993) Design applications of genetic algorithms. in SPE Annual Technical Conference and Exhibition. Society of Petroleum Engineers.

Jiang, H., et al. (2013). Density and surface tension of pure ionic liquid 1-butyl-3-methyl-imidazolium l-lactate and its binary mixture with alcohol and water. *The Journal of Chemical Thermodynamics, 64*, 1–13.

Kardani, M. N., et al. (2018). Group contribution methods for estimating CO2 absorption capacities of imidazolium and ammonium-based polyionic liquids. *Journal of Cleaner Production, 203*, 601–618.

Kardani, M. N., et al. (2019). Phase behavior modeling of asphaltene precipitation utilizing RBF-ANN approach. *Petroleum Science and Technology, 37*(16), 1861–1867.

Kardani, M. N., & Baghban, A. (2017). Utilization of LSSVM strategy to predict water content of sweet natural gas. *Petroleum Science and Technology, 35*(8), 761–767.

Karimipour, A., et al. (2018). Synthesized CuFe2O4/SiO2 nanocomposites added to water/EG: evaluation of the thermophysical properties beside sensitivity analysis & EANN. *International Journal of Heat and Mass Transfer, 127*, 1169–1179.

Karimipour, A., et al. (2019). A novel nonlinear regression model of SVR as a substitute for ANN to predict conductivity of MWCNT-CuO/water hybrid nanofluid based on empirical data. *Physica A: Statistical Mechanics and its Applications, 521*, 89–97.

Kermanpour, F., & Niakan, H. (2012). Measurement and modeling the excess molar properties of binary mixtures of [C6mim][BF4]+ 3-amino-1-propanol and {[C6mim][BF4]+ isobutanol}: Application of Prigogine–Flory–Patterson theory. *The Journal of Chemical Thermodynamics, 48*, 129–139.

Keykhosravi, A., Simjoo, M. (2018) Application of gamma-alumina nanoparticles to enhance spontaneous imbibition in low permeable, oil-wet carbonate rocks. in 80th EAGE Conference and Exhibition 2018. 2018. European Association of Geoscientists & Engineers.

Keykhosravi, A., & Simjoo, M. (2019). Insights into stability of silica nanofluids in brine solution coupled with rock wettability alteration: An enhanced oil recovery study in oil-wet carbonates. *Colloids and Surfaces A: Physicochemical and Engineering Aspects, 583*, 124008.

Keykhosravi, A., & Simjoo, M. (2020). Enhancement of capillary imbibition by Gamma-Alumina nanoparticles in carbonate rocks: Underlying mechanisms and scaling analysis. *Journal of Petroleum Science and Engineering, 187*, 106802.

Lashkarblooki, M., et al. (2012). Viscosity prediction of ternary mixtures containing ILs using multilayer perceptron artificial neural network. *Fluid Phase Equilibria, 326*, 15–20.

Lashkarbolooki, M. (2017). Artificial neural network modeling for prediction of binary surface tension containing ionic liquid. *Separation Science and Technology, 52*(8), 1454–1467.

Lashkarbolooki, M., Hezave, A. Z., & Ayatollahi, S. (2012). Artificial neural network as an applicable tool to predict the binary heat capacity of mixtures containing ionic liquids. *Fluid Phase Equilibria, 324*, 102–107.

Lashkarbolooki, M., Hezave, A. Z., & Babapoor, A. (2013). Correlation of density for binary mixtures of methanol+ ionic liquids using back propagation artificial neural network. *Korean Journal of Chemical Engineering, 30*(1), 213–220.

Lazzús, J. A., et al. (2017). Estimating the temperature-dependent surface tension of ionic liquids using a neural network-based group contribution method. *Industrial & Engineering Chemistry Research, 56*(23), 6869–6886.

Liu, Y., et al. (2016). Adsorption behavior of low-concentration imidazolium-based ionic liquid surfactant on silica nanoparticles. *Langmuir, 32*(11), 2582–2590.

Low, K., Kobayashi, R., & Izgorodina, E. I. (2020). The effect of descriptor choice in machine learning models for ionic liquid melting point prediction. *The Journal of Chemical Physics, 153*(10), 104101.

Machida, H., et al. (2010). Measurement and correlation of high pressure densities of ionic liquids, 1-Ethyl-3-methylimidazolium l-Lactate ([emim][Lactate]), 2-Hydroxyethyl-trimethylammonium l-Lactate ([(C2H4OH)(CH3) 3N][Lactate]), and 1-Butyl-3-methylimidazolium chloride ([bmim][Cl]). *Journal of Chemical & Engineering Data, 56*(4), 923–928.

Majumder, P., Majumder, M., & Saha, A. K. (2019). Real-time monitoring of power production in modular hydropower plant: most significant parameter approach. *Environment, Development and Sustainability*. https://doi.org/10.1007/s10668-019-00369-6.

Mallard, W., Linstrom P. (2000) NIST Chemistry WebBook, NIST Standard Reference Database Number 69. Gaithersburg, MD, **20899.**

Mohanraj, M., Jayaraj, S., & Muraleedharan, C. (2015). Applications of artificial neural networks for thermal analysis of heat exchangers: A review. *International Journal of Thermal Sciences, 90*, 150–172.

Moradikazerouni, A., et al. (2019). Assessment of thermal conductivity enhancement of nano-antifreeze containing single-walled carbon nanotubes: Optimal artificial neural network and curve-fitting. *Physica A: Statistical Mechanics and its Applications, 521*, 138–145.

Mosallanejad, M. R., Khosravi-Nikou, M. R., & Shaahmadi, F. (2018). Liquid-liquid extraction of alcohols from their azeotropic mixtures with hexane using ionic liquid. *Journal of Chemical & Engineering Data, 63*(9), 3482–3487.

Mulero, Á., Cachadiña, I., & Valderrama, J. O. (2017). Artificial neural network for the correlation and prediction of surface tension of refrigerants. *Fluid Phase Equilibria, 451*, 60–67.

Nabipour, N., et al. (2020). Estimating biofuel density via a soft computing approach based on intermolecular interactions. *Renewable Energy, 152*, 1086–1098.

Nazari, S., et al. (2020). A novel technique based on artificial intelligence for modeling the required temperature of a solar bread cooker equipped with concentrator through experimental data. *Food and Bioproducts Processing, 123*, 437–449.

Nguyen, H., Bui, X.-N., & Moayedi, H. (2019). A comparison of advanced computational models and experimental techniques in predicting blast-induced ground vibration in open-pit coal mine. *Acta Geophysica*. https://doi.org/10.1007/s11600-019-00304-3.

Oliveira, M., et al. (2012). Surface tension of binary mixtures of 1-alkyl-3-methylimidazolium bis (trifluoromethylsulfonyl) imide ionic liquids: experimental measurements and soft-SAFT modeling. *The Journal of Physical Chemistry B, 116*(40), 12133–12141.

Oz, E., et al. (2020). Surface propensity of anions in a binary ionic liquid mixture assessed by full-range angle-resolved-XPS and surface tension measurements. *Chemphyschem: a European Journal of Chemical Physics and Physical Chemistry*. https://doi.org/10.1002/cphc.202000750.

Park, J., & Sandberg, I. W. (1991). Universal approximation using radial-basis-function networks. *Neural computation, 3*(2), 246–257.

Peng, Y., et al. (2020). Develop optimal network topology of artificial neural network (AONN) to predict the hybrid nanofluids thermal conductivity according to the empirical data of Al2O3–Cu nanoparticles dispersed in ethylene glycol. *Physica A: Statistical Mechanics and its Applications*. https://doi.org/10.1016/j.physa.2019.124015.

Qu, S., Zhao, L., & Xiong, Z. (2020). Cross-layer congestion control of wireless sensor networks based on fuzzy sliding mode control. *Neural Computing and Applications*. https://doi.org/10.1007/s00521-020-04758-1.

Rao, R. V., Savsani, V. J., & Vakharia, D. (2012). Teaching–learning-based optimization: an optimization method for continuous non-linear large scale problems. *Information Sciences, 183*(1), 1–15.

Rilo, E., et al. (2009). Density and surface tension in binary mixtures of CnMIM-BF4 ionic liquids with water and ethanol. *Fluid Phase Equilibria, 285*(1–2), 83–89.

Rilo, E., et al. (2012). Surface tension of four binary systems containing (1-ethyl-3-methyl imidazolium alkyl sulphate ionic liquid+ water or+ ethanol). *The Journal of Chemical Thermodynamics, 49*, 165–171.

Romero, C., & Carter, J. (2001). Using genetic algorithms for reservoir characterisation. *Journal of Petroleum Science and Engineering, 31*(2–4), 113–123.

Rumelhart, D. E., Hinton, G. E., & Williams, R. J. (1986). Learning representations by back-propagating errors. *Nature*. https://doi.org/10.1038/323533a0.

Safaei, M. R., et al. (2019). Evaluating the effect of temperature and concentration on the thermal conductivity of ZnO-TiO2/EG hybrid nanofluid using artificial neural network and curve fitting on experimental data. *Physica A: Statistical Mechanics and its Applications, 519*, 209–216.

Schilling, R. J., Carroll, J. J., & Al-Ajlouni, A. F. (2001). Approximation of nonlinear systems with radial basis function neural networks. *IEEE Transactions on Neural Networks, 12*(1), 1–15.

Seki, S., et al. (2012). Comprehensive refractive index property for room-temperature ionic liquids. *Journal of Chemical & Engineering Data, 57*(8), 2211–2216.

Shaahmadi, F., Hashemi Shahraki, B., & Farhadi, A. (2018). Liquid–liquid extraction of toluene from its mixtures with aliphatic hydrocarbons using an ionic liquid as the solvent. *Separation Science and Technology*. https://doi.org/10.1080/01496395.2018.1449859.

Shojaeian, A. (2019). Surface tension measurements of aqueous 1-alkyle-3-methylimidazolume tetrafluoroborate [Cnmim][BF4](n= 2, 4, 6) solutions and modeling surface tension of ionic liquid binary mixtures using six various models. *Thermochimica Acta, 673*, 119–128.

Shojaeian, A., & Asadizadeh, M. (2020). Prediction of surface tension of the binary mixtures containing ionic liquid using heuristic approaches; An input parameters investigation. *Journal of Molecular Liquids, 298*, 111976.

Soleimani, R., et al. (2018). Toward an intelligent approach for predicting surface tension of binary mixtures containing ionic liquids. *Korean Journal of Chemical Engineering, 35*(7), 1556–1569.

Tajikmansori, A., Hosseini, M., & Dehaghani, A. H. S. (2020). Mechanistic study to investigate the injection of surfactant assisted smart water in carbonate rocks for enhanced oil recovery: An experimental approach. *Journal of Molecular Liquids*. https://doi.org/10.1016/j.molliq.2020.114648.

Tariq, M., et al. (2012). Surface tension of ionic liquids and ionic liquid solutions. *Chemical Society Reviews, 41*(2), 829–868.

Troncoso, J., et al. (2006). Thermodynamic properties of imidazolium-based ionic liquids: densities, heat capacities, and enthalpies of fusion of [bmim][PF6] and [bmim][NTf2]. *Journal of Chemical & Engineering Data, 51*(5), 1856–1859.

Vakili-Nezhaad, G., et al. (2012). Effect of temperature on the physical properties of 1-butyl-3-methylimidazolium based ionic liquids with thiocyanate and tetrafluoroborate anions, and 1-hexyl-3-methylimidazolium with tetrafluoroborate and hexafluorophosphate anions. *The Journal of Chemical Thermodynamics, 54*, 148–154.

Vanani, M. B., Daneshfar, R., & Khodapanah, E. (2019). A novel MLP approach for estimating asphaltene content of crude oil. *Petroleum Science and Technology, 37*(22), 2238–2245.

Vega, L. F., et al. (2010). Modeling ionic liquids and the solubility of gases in them: recent advances and perspectives. *Fluid Phase Equilibria, 294*(1–2), 15–30.

Wandschneider, A., Lehmann, J. K., & Heintz, A. (2008). Surface tension and density of pure ionic liquids and some binary mixtures with 1-propanol and 1-butanol. *Journal of Chemical & Engineering Data, 53*(2), 596–599.

Wang, J.-Y., et al. (2011b). Thermophysical properties of pure 1-ethyl-3-methylimidazolium methylsulphate and its binary mixtures with alcohols. *Fluid Phase Equilibria, 305*(2), 114–120.

Wang, J.-Y., et al. (2011a). Density and surface tension of pure 1-ethyl-3-methylimidazolium L-lactate ionic liquid and its binary mixtures with water. *The Journal of Chemical Thermodynamics, 43*(5), 800–804.

Wang, Z., Song, Z., & Zhou, T. (2021). Machine learning for ionic liquid toxicity prediction. *Processes, 9*(1), 65.

Wei, Y., et al. (2010). Physicochemical property estimation of an ionic liquid based on glutamic acid−BMI-Glu. *Journal of Chemical & Engineering Data, 55*(7), 2616–2619.

Wu, H., et al. (2019). Present a new multi objective optimization statistical Pareto frontier method composed of artificial neural network and multi objective genetic algorithm to improve the pipe flow hydrodynamic and thermal properties such as pressure drop and heat transfer coefficient for non-Newtonian binary fluids. *Physica A: Statistical Mechanics and its Applications, 535*, 122409.

Yao, X., et al. (2004). Comparative study of QSAR/QSPR correlations using support vector machines, radial basis function neural networks, and multiple linear regression. *Journal of Chemical Information and Computer Sciences, 44*(4), 1257–1266.

Yildiz, A. R. (2013). Optimization of multi-pass turning operations using hybrid teaching learning-based approach. *The International Journal of Advanced Manufacturing Technology, 66*(9–12), 1319–1326.
Zendehboudi, S., et al. (2012). Prediction of condensate-to-gas ratio for retrograde gas condensate reservoirs using artificial neural network with particle swarm optimization. *Energy & Fuels, 26*(6), 3432–3447.
Zendehboudi, S., et al. (2013). Thermodynamic investigation of asphaltene precipitation during primary oil production: Laboratory and smart technique. *Industrial & Engineering Chemistry Research, 52*(17), 6009–6031.
Zendehboudi, S., et al. (2014). Estimation of breakthrough time for water coning in fractured systems: Experimental study and connectionist modeling. *AIChE Journal, 60*(5), 1905–1919.
Zhu, Q. (2019). Research on road traffic situation awareness system based on image big data. *IEEE Intelligent Systems, 35*(1), 18–26.